ELSEVIER

Journal of Biomechanics 38 (2005) 1822–1829

JOURNAL OF BIOMECHANICS

www.elsevier.com/locate/jbiomech
www.JBiomech.com

Optimal compliant-surface jumping: a multi-segment model of springboard standing jumps

Kuangyou B. Cheng, Mont Hubbard*

Sports Biomechanics Laboratory, Department of Mechanical and Aeronautical Engineering, University of California, Davis, CA 95616, USA

Accepted 22 August 2004

Abstract

A multi-segment model is used to investigate optimal compliant-surface jumping strategies and is applied to springboard standing jumps. The human model has four segments representing the feet, shanks, thighs, and trunk–head–arms. A rigid bar with a rotational spring on one end and a point mass on the other end (the tip) models the springboard. Board tip mass, length, and stiffness are functions of the fulcrum setting. Body segments and board tip are connected by frictionless hinge joints and are driven by joint torque actuators at the ankle, knee, and hip. One constant (maximum isometric torque) and three variable functions (of instantaneous joint angle, angular velocity, and activation level) determine each joint torque. Movement from a nearly straight motionless initial posture to jump takeoff is simulated. The objective is to find joint torque activation patterns during board contact so that jump height can be maximized. Minimum and maximum joint angles, rates of change of normalized activation levels, and contact duration are constrained. Optimal springboard jumping simulations can reasonably predict jumper vertical velocity and jump height. Qualitatively similar joint torque activation patterns are found over different fulcrum settings. Different from rigid-surface jumping where maximal activation is maintained until takeoff, joint activation decreases near takeoff in compliant-surface jumping. The fulcrum–height relations in experimental data were predicted by the models. However, lack of practice at non-preferred fulcrum settings might have caused less jump height than the models' prediction. Larger fulcrum numbers are beneficial for taller/heavier jumpers because they need more time to extend joints.
© 2004 Elsevier Ltd. All rights reserved.

Keywords: Optimization; Jumping; Surface compliance; Muscular activation; Diving

1. Introduction

Strategies of maximum height rigid-surface jumping have been studied by models with increasing complexity (Levine et al., 1983a, b; Pandy et al., 1990; Soest et al., 1993). Joint kinematics, ground reaction forces, and muscle EMG have been experimentally recorded (e.g. Bobbert and Ingen Schenau, 1988). Other researchers approached running high- and long-jump characteristics using extremely simple models (Alexander, 1990; Seyfarth et al., 1999, 2000). Only a few studies considered maximum-height jumping from compliant surfaces. Sanders and Wilson (1992) and Sanders and Allen (1993) experimentally investigated surface compliance effects on drop jumping (dropping from a height onto a surface, then jumping for maximum height) but, to the best of our knowledge, only one study (Cheng and Hubbard, 2004) has concerned maximum-height jumping initiated from a compliant surface. Although a one-dimensional (1-D) lumped mass and massless leg model was able to explain some of the characteristics in multi-segment human jumping, it was not entirely adequate.

Two-dimensional (2-D) models of compliant-surface jumping should be considered, especially in diving jumping in which the board tip undergoes not only vertical but horizontal movement. Two kinds of springboard diving are performed in competitions. In standing

*Corresponding author. Tel.: +530 752 6450; fax: +530 752 4158
E-mail address: mhubbard@ucdavis.edu (M. Hubbard).

0021-9290/$ - see front matter © 2004 Elsevier Ltd. All rights reserved.
doi:10.1016/j.jbiomech.2004.08.023

dives, the diver begins at the tip and maintains contact until takeoff. However, in running dives, the diver takes several steps to the board tip, executes a hurdle jump, and re-catches the board for takeoff.

Diving springboard stiffness can be adjusted using fulcrum settings between 1 (stiffest) and 9 (softest). Linear and rotational mass–spring models for springboard were examined (Sprigings et al., 1989, 1990; Kooi and Kuipers, 1994) as well as springboard kinetics (Miller, 1983) and tip kinematics (Jones et al., 1993; Jones and Miller, 1996; Miller et al., 1998). However, most studies focused on running-dive kinematics including vertical velocity (Miller and Munro, 1984, 1985) and angular momentum (Sanders and Wilson, 1987; Miller and Sprigings, 2001), rather than studying how surface compliance would change jumping strategies. Although Boda (1993) used regression analysis to identify optimal standing dive fulcrum settings, the underlying body coordination was not addressed.

Only two studies have specifically considered standing-dive coordination strategies (Cheng and Hubbard, 2004; Sprigings and Watson, 1983) in spite of reasonably well-understood running-dive kinematics. However, 1-D models were used in both studies and the latter even neglected leg action. Validity of a rotational mass-spring rigid-bar springboard model has been established (Kooi and Kuipers, 1994), but diver–board force interaction has not been carefully examined. Moreover, although divers have preferred fulcrum settings, it is not clear if they are biased toward a preferred one due to lack of practice at other settings. Simulation is the way to test whether optimal fulcrum settings in standing dives actually exist. The purpose of this study is to investigate compliant-surface jumping strategies (joint torque activation patterns) by using a multi-segment model with springboard jumping for experimental comparison. We hypothesize that: (1) general coordination patterns exist for maximizing jump height different from those in rigid-surface jumping; (2) jump height depends on fulcrum setting (which determines board stiffness) and the best setting differs among divers.

2. Materials and methods

A Maxiflex "B" springboard was previously characterized by a 1-D mass–spring model. Equivalent board mass m_b and stiffness k for fulcrum settings $S = 1$, 5, and 9 were measured by Sprigings et al. (1990) and interpreted by Miller et al. (1998). Cubic spline interpolations for m_b and k at other settings were calculated (Cheng and Hubbard, 2004). However, in order to model both the horizontal and vertical board tip motion, a rotational mass–spring system which simulated board tip motion accurately (Kooi and Kuipers, 1994) is used in the present study. Fig. 1 shows

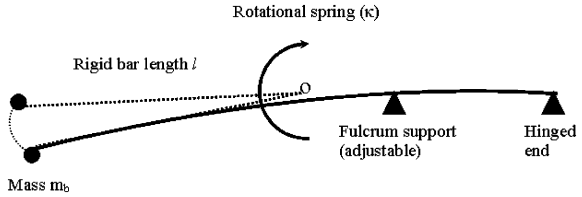

Fig. 1. Real springboard and the rotational mass–spring rigid bar model (dashed). Real board stiffness can be adjusted by moving the fulcrum support horizontally. The rigid bar (modeled springboard) is hinged at point O, which is the point of intersection of the perpendicular bisector of O to loaded and unloaded board (Kooi and Kuipers, 1994).

Table 1
Equivalent board mass and stiffness dependence on fulcrum number

Fulcrum	1	3	5	7	9
m_b (kg)	6.32	6.5389	6.7656	7.00	7.2422
l (m)	2.53	2.6189	2.7089	2.80	2.8922
κ (N m)	38877	39148.3	39366.3	39531	39642.3

a real springboard and the modeled board. The equivalent board mass ($m_b = 7.00$ kg), bar length ($l = 2.80$ m), and rotational spring constant ($\kappa = 39\,531$ N m) generate a vertical board tip displacement equivalent to fulcrum setting = 7, while the values ($m_b = 6.32$ kg; $l = 2.53$ m; $\kappa = 38\,877$ N m/rad) correspond to fulcrum setting = 1 in the 1-D model. Cubic splines interpolate corresponding m_b, l, and κ at other fulcrum settings (Table 1).

A planar four-segment human model with frictionless revolute joints and joint torque actuators is used to simulate springboard standing jumps. To investigate the sensitivity of jump height and torque activation patterns to a jumper's size, calculations are done for two jumpers' mass and length parameters specified in the Appendix. The model performing a backward standing jump (Fig. 2) includes four segments representing feet, shanks, thighs, and HAT (head–arms–trunk) with joint angle definitions. The distal end of the feet is connected to the board tip by a frictionless revolute joint.

Equations of motion are derived using symbolic dynamics software AUTOLEV (Schaechter et al., 1996). Jumping simulations begin from a balanced posture which generally matches measured average initial postures, with slight differences due to a model's rigid-segment assumption. Model inputs are torques at the ankle, knee, and hip joints. Unlike a previous simulation study (Selbie and Caldwell, 1996) in which joints only extend or relax, we assume that joints can actively extend, relax, or flex. Active joint torques represent total contributions of joint flexors and extensors.

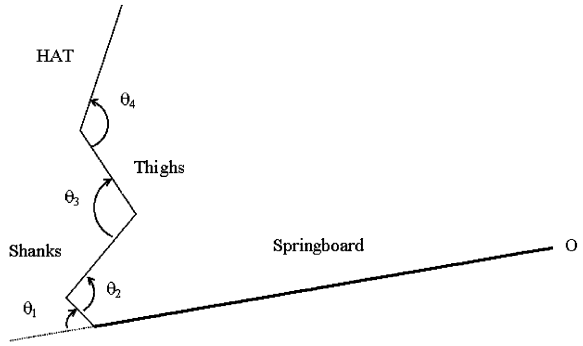

Fig. 2. The human model has four segments connected by frictionless revolute joints. The toe tip is also connected to the board tip by a frictionless revolute joint. All positions are measured relative to point O.

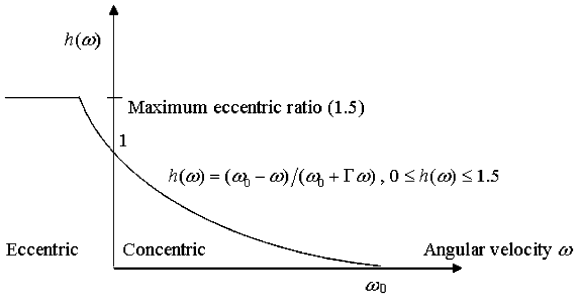

Fig. 3. Angular velocity dependence $h(\omega)$ for extension joint activation ($A(t)>0$). The dependence is decreased to zero when ω exceeds its maximum ω_0. If $\omega<0$ (and $A(t)>0$), $h(\omega)$ increases to a saturation value 1.5, which effectively models eccentric muscle contraction. Similar relations also hold for negative ω_0 when $A(t)<0$ (flexion joint activation).

Each active joint torque T is the product of maximum torque $T_{\max}$ and three variable factors: angle dependence $f(\theta)$, angular velocity dependence $h(\omega)$, and activation level $A(t)$ depending on time t:

$$T = T_{\max} \times f(\theta) \times h(\omega) \times A(t). \quad (1)$$

Values of $T_{\max}$ at the knee were measured for both our subjects. Due to the difficulty in measuring $T_{\max}$ at other joints, the values are assigned using the ratios in a previous study (Selbie and Caldwell, 1996). Thus, the male model's $T_{\max} = 550$, 500, and 600 N m at ankle, knee, and hip, respectively, while the female's $T_{\max}$ values are half of those in the male model. Angle dependence $f(\theta)$ is from Pandy et al. (1990) and Hoy et al. (1990) for extension and flexion, respectively. Angular velocity dependence $h(\omega)$ is (Selbie and Caldwell, 1996)

$$h(\omega) = \begin{cases} (\omega_0 - \omega)/(\omega_0 + \Gamma\omega), & \frac{\omega}{\omega_0} < 1, \\ 0, & \frac{\omega}{\omega_0} \geqslant 1, \end{cases} \quad (2)$$

where ω is the instantaneous joint angular velocity (positive meaning joint extension), ω_0 is the maximum joint angular velocity in extension (positive) or flexion (negative), and Γ is a constant representing a shape factor. In the male model, $\omega_0 = \pm 20$ rad/s (Selbie and Caldwell, 1996). The female value is increased to $\omega_0 = \pm 21.95$ rad/s by the inverse square root of the height ratio (Alexander, 1990). $\Gamma = 2.5$ for both models. If the signs of $\omega(t)$ and $A(t)$ are different (which is similar to eccentric muscle contraction), $h(\omega)$ can be increased to a saturation value 1.5 (Fig. 3).

The activation levels $A(t)$ at each joint characterize the coordination strategy. To reduce computational effort, $A(t)$ is approximated by a cubic spline fit of nine nodal values. The inputs of each simulation include an assumed final time and nine nodal $A(t)$ values at times equally spaced throughout board contact, with the first at the initial time and the last at takeoff. Nine nodes suffice since doubling the number increases jump height by less than 0.4 cm. The fixed initial nodes correspond to static equilibrium. Positive and negative $A(t)$ represent active extending and flexing, respectively. $A(t) = +1/-1$ means full effort joint extension/flexion. The derivative dA/dt must be constrained based on typical muscle activation and deactivation times of 20 and 200 ms, respectively (Pandy et al., 1990). A single value (80 ms) somewhat lower than the mean is assumed since muscle activation should dominate board contact period. Thus, $|dA/dt|$ cannot exceed $1/0.08\ s^{-1}$.

The control goal is to maximize jump height J_0:

$$J_0 = (y_f + v_f^2/2g), \quad (3)$$

where y_f and v_f are the jumper center of mass (c.m.) takeoff vertical position and velocity. Since different takeoff times t_f result from different joint torque patterns (actually nodal torque activations), t_f is also a control variable (Bryson, 1999). Maximizing J_0 is subject to state and control constraints. In optimal torque activation calculations, nodal activation is not constrained formally. Rather, $A(t)$ is truncated when it lies outside [−1, 1]. The terminal time is constrained by $t_f < 1.5$ s, since experimental data show that maximal board depression duration is about 0.5 s, and longer durations may result in "excessive" flexion/extension oscillations before takeoff. This is prohibited by the rules (NCAA, 2001): "the diver must not rock the board excessively or lift their feet from the board before takeoff". Force from the board on the toe is constrained to be upward. Other constraints are the takeoff condition that requires zero vertical board reaction force at takeoff and joint angle constraints to prevent joint hyperextension. Only the ankle joint angle constraint (>1 rad) was found to be active.

To maximize the likelihood of finding the global rather than a local maximum, the genetic algorithm (Belegundu and Chandrupatla, 1999) is used first. Combined with the downhill simplex method (Nelder and Mead, 1965; Press, 1997), optimal solutions are found more confidently.

Jumping of one male and one female diver on a Maxiflex "B" springboard was used for experimental comparisons. Both divers had about 1 year of experience with preferred standing dive fulcrum settings $S = 3.5$ and 4, respectively. After their informed consent and approval by the University Human Subjects Research Review Committee were obtained, they performed two maximal-height backward standing dive jumps at $S = 1$, 5, and 9. Subjects were asked to start from a balanced motionless posture and perform only one maximum joint flexion–extension before takeoff. Three high-speed cameras (240 Hz) and a motion analysis (Motion Analysis, Eva 7.0, Santa Rosa, CA) system recorded and determined positions of six reflective markers at the board tip, fifth metatarsal, ankle, knee, hip, and shoulder. Divers jumped onto a mat on top of a tethered raft because water entry could affect the marker's position. Arm-motion effects were eliminated by holding the arms tightly against the chest.

3. Results

Results from a simulated optimal and actual male diving jump ($S = 5$) are compared (Figs. 4–6 and Table 2). Optimal contact duration is 0.852 s. Optimal simulated results agree reasonably well with experiments but some discrepancies exist. Since divers' performance might not be optimal due to lack of proficiency in the required configuration, experimental results are included for a general comparison but exact agreement with simulation should not be expected. Although subjects were asked to perform only one maximum joint flexion–extension before takeoff, small oscillations from ankle movement were observed in all jumps, causing difficulty in determining the start time. Conversely, takeoff time is unambiguous in both experiment and simulation. Therefore, takeoff time t_f is set to zero and the start time is specified using the simulated duration. Major discrepancies in simulated and measured results are maximum board tip depression, takeoff horizontal velocity, and joint angular kinematics before maximal depression (Figs. 4–6). Possible reasons for discrepancies are addressed in the Discussion section.

Both simulated optimal and measured results (across different fulcrum settings) suggest a general movement pattern for achieving maximum height, and the simulations show clearly that joint activation patterns are different from those in rigid-surface jumping. All simulations show partial joint extension

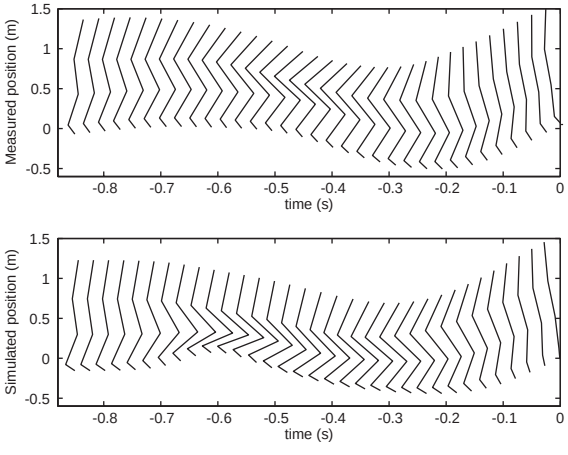

Fig. 4. Measured and simulated jumper's position vs. time. Because of the difficulty in determining the start time in real jumps due to small ankle movements, simulated contact duration is used to specify contact duration in the measured jump. Horizontal displacement of the board tip is not shown here.

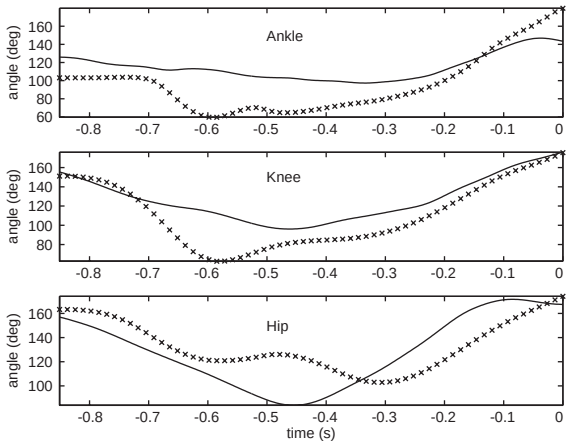

Fig. 5. Jumper ankle, knee, and hip angular displacement vs. time; measured (—) and simulated (x). Simulated minimum ankle and knee angles are smaller than measured angles, but simulated minimum hip angle is larger than the measured result.

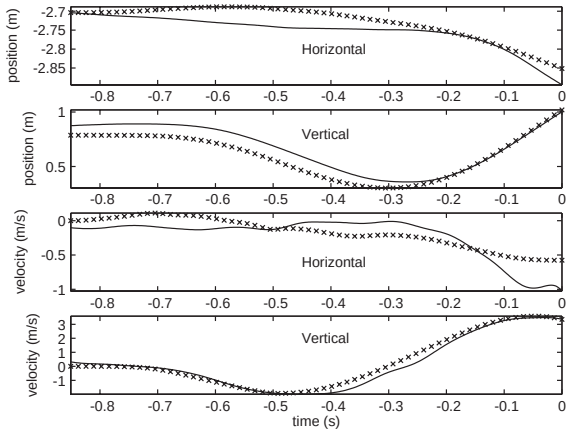

Fig. 6. Jumper c.m. horizontal and vertical position and velocity vs. time; measured (—) and simulated (x). Because simulated contact duration is used to specify that in the measured jump, measured initial horizontal/vertical velocity is not zero in the figure. Except for the horizontal velocity, there is general agreement between measured and simulated results.

Table 2
Features of actual and optimal simulated jumps shown in Fig. 4

	Actual	Simulated
Max. board tip depression (m)	0.502	0.448
Min. jumper c.m. vertical velocity (m/s)	−1.993	−1.933
Takeoff vertical c.m. velocity (m/s)	3.356	3.353
Takeoff horizontal c.m. velocity (m/s)	−1.026	−0.577
Max. jumper c.m. flight height (m)	1.560	1.593

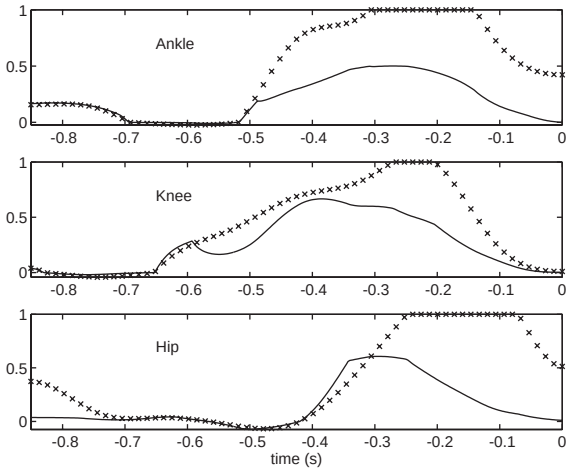

Fig. 7. Simulated joint torque (—) and joint activation level (x). Joint torque is normalized by dividing its value by maximum isometric torque. The relaxation–flexion–extension torque pattern is found in all three joints across all fulcrum settings. The sudden depression in knee torque shortly after −0.6 s is due to the angular velocity dependence effect (Fig. 3) corresponding to the transition from flexion to extension. The hip joint has the most obvious active flexion (negative activation level).

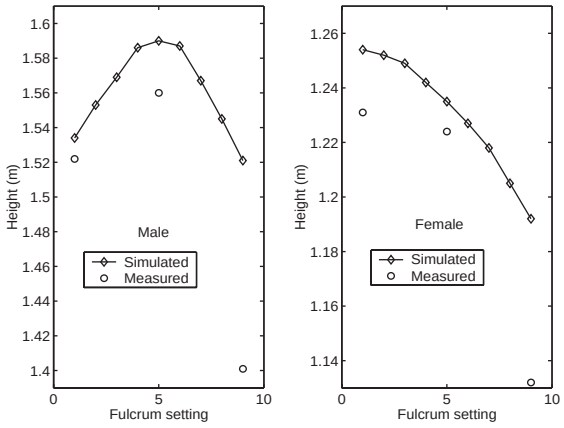

Fig. 8. Simulated and measured male and female jump height vs. fulcrum setting S. The simulated height–fulcrum relation generally agrees with the measured one except at $S=9$.

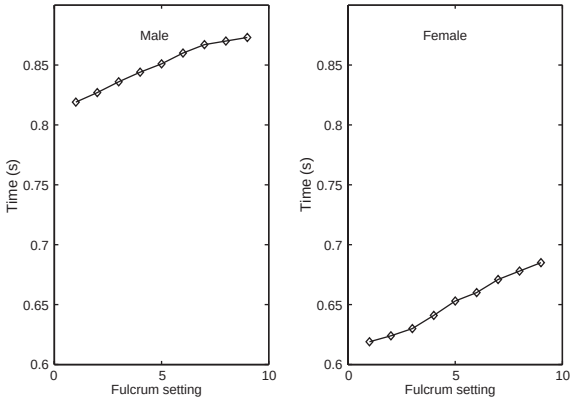

Fig. 9. Simulated male and female contact time increases with fulcrum setting S.

torque activation followed by slight flexion activation and maximal extension activation. This strategy is similar to countermovement rigid-surface jumping (Pandy et al., 1990). However, joint activation at takeoff decreases especially in the knee (Fig. 7) instead of remaining at maximal activation (Selbie and Caldwell, 1996; Cheng and Hubbard, 2003).

Simulations suggest a specific maximum-height fulcrum setting for divers (Fig. 8), and seem to agree with the shape of the measured height–fulcrum relation. Both the optimal simulated results and our limited experimental data show that the male jumps highest at $S=5$ and the female jumps highest at $S=1$. However, there is larger difference in the jump height at $S=9$ for both jumpers. Contact time increases with S for all simulated cases and the male model has longer duration (Fig. 9).

Comparison of the male and female height–fulcrum relation suggests that the best (maximum-height) fulcrum setting differs among divers (Fig. 8). Since only two sets of body parameters were used, extra simulations were done for a new model taller and heavier than the male model. Segment anthropometric parameters are from averaged data (Winter, 1990) of a 1.9 m, 90 kg male. The simulated height–fulcrum relation of the new model is different from the previous two, and maximum height occurred at $S=7$.

4. Discussion

The model in the present study is actuated by independent joint torques neglecting muscle biarticularity and tendon elasticity. Although biarticular muscles are important in jumping (e.g. gastrocnemius can increase jump height by as much as 25%), the increase is not due to the biarticularity since jumping performance is similar if gastrocnemius is replaced with a uniarticular ankle plantarflexor (Pandy and Zajac, 1991). Soest et al. (1993) also showed that jump height decreased by only 10 mm when gastrocnemius was changed to be uniarticular. Moreover, models similar to the present one have been validated in gymnastic

tumbling (King and Yeadon, 2004) in which the inclusion of series elastic element at the ankle joint was shown to improve the agreement between actual and simulated movement by less than 2% (Yeadon and King, 2002). In our previous one-joint approach (Cheng and Hubbard, 2004), simulations were first performed with and without series elastic compliance, but very little difference was found in terms of jump height and knee torque patterns.

The general agreement between simulated and measured results shows the model's ability to make reasonable predictions of diver c.m. velocities and jump height, even though the entire diver–board interaction kinematics are not exactly reproduced. The discrepancy in maximum board tip depression is probably due to different initial conditions in simulations and experiments. Zero initial velocities are assumed in simulations. In real jumps, however, joint torques required for active posture control cause small board and ankle motions, even though subjects were asked to start jumping from a motionless posture. Non-zero initial board tip velocity undoubtedly leads to larger board depression and may be partially responsible for the discrepancy in initial joint angular kinematics. The discrepancies in horizontal velocity and joint angular kinematics near takeoff are probably due to jumpers' non-optimal performance. Since jumpers wanted to land safely on the mat on top of a tethered raft, they tended to increase backward velocity near takeoff and decrease joint angular velocity so that an upright posture could be maintained after takeoff. On the contrary, the model concerns only maximizing jump height without flight and landing considerations. Thus, simulated backward velocity was smaller and joint angles kept increasing near takeoff. Previous studies (Pandy et al., 1990; Soest et al., 1993) also showed increasing joint angular displacement near takeoff.

Although each joint generally exhibits the activation pattern of relaxation, minor flexion, and full and partial extension (Fig. 7), some differences exist among joints. The ankle has the longest initial partial extension, probably because it serves to excite board oscillation to gain more potential energy. The knee relaxes almost immediately after the start and reaches full extension most slowly, which can amplify board oscillation magnitude. The hip has the largest flexion activation and reaches full extension the latest. Both the relaxing knee and flexing hip cause negative knee and hip angular velocities and allow eccentric muscle contraction at the beginning of upward thrust. This special optimal joint torque activation pattern is not expected to appear in our subjects due to their lack of proficiency in the required jumping configuration. This is another possible reason for the discrepancy in joint angular kinematics between simulation and measurements.

Surface compliance changes torque activation strategies in jumping considerably. In compliant-surface jumping, maximal joint activation occurs around maximal board deflection when the board is best able to resist (Figs. 4 and 7). Not as much muscular work can be done if full joint activation is timed too early or late. In rigid-surface jumping, however, jump height is maximized by maintaining full joint activation to achieve maximum joint angular velocity, which results in zero joint torque and zero ground reaction force at takeoff. Moreover, a straight posture is not achieved at takeoff (Selbie and Caldwell, 1996) and joint extension continues during flight. But in springboard jumping, takeoff occurs with a nearly straight body, which is required to "ride" the board just before takeoff, simultaneously extracting as much of its energy as possible and maximizing the c.m. height at takeoff.

Similar to Selbie and Caldwell (1996), knee activation is found to lead the other two joints, which seems to contradict the proximal-to-distal segment coordination sequencing in jumps without countermovement (Bobbert and Ingen Schenau, 1988). As was explained by Selbie and Caldwell (1996), this discrepancy is due to the need for re-adjusting the c.m. position to a favorable position prior to joint extension activation.

Both simulated and measured fulcrum–height relations suggest a subject-specific maximum-height fulcrum setting (Fig. 8). Predicted jump height at $S = 9$ does not agree with experiments as well as those at low fulcrum settings ($S \leqslant 5$). Since subjects' preferred settings are at $S = 3.5$ *and* 4, lack of practice could be the reason for the larger jump height discrepancy at $S = 9$. The predicted increase of optimal fulcrum setting with increasing jumper mass and length is reasonable. Larger jumpers require more time for joint extension and this is provided by a lower board–jumper natural frequency, $\omega = \sqrt{k/m}$, since equivalent vertical board stiffness k decreases with S.

This fulcrum–height relation may seem to contradict some researchers' assumptions. Jones and Miller (1996) stated that theoretically larger vertical velocity can be generated using larger S. Boda (1993) argued that if a diver could relax and wait for the springboard, the looser setting (higher fulcrum number) might result in more height. However, with the additional model, it could be inferred that high fulcrum numbers are optimal for tall jumpers, which agrees with previous arguments. We also believe that since maximizing jump height involves fast joint extension, a loose springboard has too long a rebound time for shorter jumpers to push on. Thus only tall jumpers can effectively take the advantage of a loose board. This argument is supported by our previous study (Cheng and Hubbard, 2004) in which longer legs and a larger range of motion correspond to higher optimal fulcrum numbers.

5. Conclusions

Optimal simulated springboard jumping results agree reasonably well with experiments with expected minor discrepancies. Simulated joint torque activation patterns for maximizing jump height are similar for all jumper sizes and fulcrum settings. These patterns include partial extension activation, slight flexion activation, and maximal extension activation timed around maximal board depression. Contrary to rigid-surface jumping, joint activation is decreased near takeoff, especially in the knee. Jump height depends on fulcrum settings with the optimal setting differing among jumpers. Larger fulcrum numbers are beneficial for taller/heavier jumpers because they need more time to extend joints.

Appendix

	Mass (kg)	Length (m)	Distal end to c.m. (m)	Moment of inertia ($kg\,m^2$)
Anthropometric parameters of the male (1.77 m *and* 83.99 kg)				
Feet	2.436	0.136	0.068	0.010
Shanks	7.810	0.404	0.229	0.116
Thighs	16.800	0.450	0.255	0.355
HAT	56.950	0.511	0.260	3.896
Anthropometric parameters of the female (1.47 m *and* 44.0 kg)				
Feet	1.276	0.111	0.055	0.007
Shanks	4.092	0.362	0.205	0.098
Thighs	8.801	0.361	0.204	0.239
HAT	29.830	0.380	0.185	1.796

References

Alexander, R.M., 1990. Optimum takeoff techniques for high and long jumps. Philosophical Transactions of the Royal Society of London B 329, 3–10.

Belegundu, A.D., Chandrupatla, T.R., 1999. Optimization Concepts and Applications in Engineering. Prentice Hall, Upper Saddle River, NJ.

Bobbert, M.F., van Ingen Schenau, G.J., 1988. Coordination in vertical jumping. Journal of Biomechanics 21, 249–262.

Boda, W.L., 1993. Predicting optimal fulcrum setting for backward takeoffs. US Diving Sport Science Seminar 1993 Proceedings, pp. 60–66.

Bryson, A.E., 1999. Dynamic Optimization. Addison-Wesley, Menlo Park, CA, p. 149.

Cheng, K.B., Hubbard, M., 2003. Simulation of optimal vertical jumps. In: Subic, A., Trivailo, P., Alam, F. (Eds.), Sports Dynamics. RMIT University, Melbourne, pp. 229–234.

Cheng, K.B., Hubbard, M., 2004. Optimal jumping strategies from compliant surfaces: a simple model of springboard standing jumps. Human Movement Science 23, 35–48.

Hoy, M.G., Zajac, F.E., Gordon, M.E., 1990. A musculoskeletal model of the human lower extremity: the effect of muscle, tendon, and moment arm on the moment–angle relationship of musculotendon actuators at the hip, knee, and ankle. Journal of Biomechanics 23, 157–169.

Jones, I.C., Miller, D.I., 1996. Influence of fulcrum position on springboard response and takeoff performance in the running approach. Journal of Applied Biomechanics 12, 383–408.

Jones, I.C., Pizzimenti, M.P., Miller, D.I., 1993. A springboard feedback system: considerations and implications for coaching. In: Malina, R., Gabriel, J.L. (Eds.), US Diving Sport Science Seminar 1993 Proceedings. US Diving Publications, Indianapolis, IN, pp. 67–79.

King, M.A., Yeadon, M.R., 2004. Maximising somersault rotation in tumbling. Journal of Biomechanics 37, 471–477.

Kooi, B.W., Kuipers, M., 1994. The dynamics of springboard. International Journal of Sport Biomechanics 10, 335–351.

Levine, W.S., Zajac, F.E., Belzer, M.R., Zomlefer, M.R., 1983a. Ankle controls that produce a maximal vertical jump when other joints are locked. IEEE Transactions on Automatic Control AC28, 1008–1016.

Levine, W.S., Christodoulou, M., Zajac, F.E., 1983b. On propelling a rod to a maximum vertical or horizontal distance. Automatica 19, 321–324.

Miller, D.I., 1983. Springboard reaction torque patterns during non-twisting dive takeoffs. In: Matsui, H., Kobayashi, K. (Eds.), Biomechanics VIII-B. Human Kinetics, Champaign, IL, pp. 822–827.

Miller, D.I., Munro, C.F., 1984. Body segment contributions to height achieved during the flight of a springboard dive. Medicine and Science in Sport and Exercise 16, 234–242.

Miller, D.I., Munro, C.F., 1985. Greg Louganis' springboard takeoff: I. Temporal and joint position analysis. International Journal of Sport Biomechanics 1, 209–220.

Miller, D.I., Sprigings, E.J., 2001. Factors influencing the performance of springboard dives of increasing difficulty. Journal of Applied Biomechanics 17, 217–231.

Miller, D.I., Osborne, M.J., Jones, I.C., 1998. Springboard oscillation during hurdle flight. Journal of Sports Sciences 16, 571–583.

NCAA, 2001. 2002 NCAA Men's and Women's Swimming and Diving Rules. National College Athletic Association. http://www.ncaa.org/library/rules/2002/2002_swim_dive_rules.pdf. Accessed 30 April 2004.

Nelder, J.A., Mead, R., 1965. A simplex method for function minimization. Computer Journal 7, 308–313.

Pandy, M.G., Zajac, F.E., 1991. Optimal muscular coordination strategies for jumping. Journal of Biomechanics 24, 1–10.

Pandy, M.G., Zajac, F.E., Sim, E., Levine, W.S., 1990. An optimal control model for maximum-height human jumping. Journal of Biomechanics 23, 1185–1198.

Press, W.H., 1997. Numerical recipes in C: the art of scientific computing, second ed. Cambridge University Press, New York. http://www.library.cornell.edu/nr/bookcpdf.html.

Sanders, R.H., Allen, J.B., 1993. Changes in net joint torques during accommodation to change in surface compliance in a drop jumping task. Human Movement Science 12, 299–326.

Sanders, R.H., Wilson, B.D., 1987. Angular momentum requirements of the twisting and nontwisting forward 1-somersault dive. International Journal of Sport Biomechanics 3, 47–62.

Sanders, R.H., Wilson, B.D., 1992. Modification of movement patterns to accommodate to a change in surface compliance in a drop jumping task. Human Movement Science 11, 593–614.

Schaechter, D.B., Levinson, D.A., Kane, T.R., 1996. AUTOLEV (Version 3).

Selbie, W.S., Caldwell, G.E., 1996. A simulation study of vertical jumping from different starting postures. Journal of Biomechanics 29, 1137–1146.

Seyfarth, A., Friedrichs, A., Wank, V., Blickhan, R., 1999. Dynamics of the long jump. Journal of Biomechanics 32, 1259–1267.

Seyfarth, A., Blickhan, R., van Leeuwen, J.L., 2000. Optimum takeoff techniques and muscle design for long jump. Journal of Experimental Biology 203, 741–750.

van Soest, A.J., Schwab, A.L., Bobbert, M.F., van Ingen Schenau, G.J., 1993. The influence of the biarticularity of the gastrocnemius muscle on vertical-jumping achievement. Journal of Biomechanics 26, 1–8.

Sprigings, E.J., Watson, L.G., 1983. A mathematical search for the optimal timing of the armswing during springboard diving take-offs. In: Winter, D.A., et al. (Eds.), BIOMECHANICS IX-B, Proceedings of the Ninth International Congress of Biomechanics. Human Kinetics, Champaign, IL, pp. 389–394.

Sprigings, E.J., Stilling, D.S., Watson, L.G., 1989. Development of a model to represent an aluminum springboard in diving. International Journal of Sport Biomechanics 5, 297–307.

Sprigings, E.J., Stilling, D.S., Watson, L.G., Dorotich, P.D., 1990. Measurement of the modeling parameters for a Maxiflex "B" springboard. International Journal of Sport Biomechanics 6, 325–335.

Winter, D.A., 1990. Biomechanics and Motor Control of Human Movement. Wiley, New York, pp. 51–63.

Yeadon, M.R., King, M.A., 2002. Evaluation of a torque-driven simulation model of tumbling. Journal of Applied Biomechanics 18, 195–206.